Proceedings of ASME Turbo Expo 2023
Turbomachinery Technical Conference and Exposition
GT2023
June 26-30, 2023, Boston, Massachusetts, USA

GT2023-101511

A Comparison of Flow Path Designs for Axial Turbines Operating with Pure CO_2 and CO_2 Mixtures

Salma I. Salah[1], Martin T. White [1,2], Abdulnaser I. Sayma[1]

[1]Thermo-Fluids Research Centre, School of Science and Technology,
City, University of London, Northampton Square, London, EC1V 0HB, United Kingdom.
[2]Thermo-Fluid Mechanics Research Centre, School of Engineering and Informatics,
University of Sussex, Falmer, Brighton, BN1 9RH.

ABSTRACT

Supercritical CO_2 (sCO_2) mixtures have been found to be promising for enhancing the performance of power cycles for concentrated solar power (CSP) applications, with up to a 6% enhancement in cycle efficiency compared to a simple recuperated CO_2 cycle depending upon the mixture and cycle configuration chosen. Given that turbine efficiency significantly affects the overall plant performance, it is important to confirm whether turbines operating with CO_2 mixtures can achieve the same efficiencies compared to pure CO_2, whilst exploring whether the use of mixtures introduces any differences in the turbine design. This study aims to investigate the differences in turbine flow path designs produced for pure CO_2 compared to CO_2 mixtures, whilst taking into account aerodynamic, rotordynamic and mechanical design aspects, as assessed during the mean-line design process. The aim of this study extends to evaluating the effect of key turbine design variables, such as the loading coefficient, flow coefficient and degree of reaction, on the flow path design and overall aerodynamic performance. Multiple flow path designs have been produced for axial turbines operating with pure CO_2 and mixtures of CO_2 with titanium tetrachloride ($TiCL_4$), hexafluorobenzene (C_6F_6) and sulphur dioxide (SO_2) for installation in a 100 MWe CSP plant. It is found that turbines operating with either pure CO_2 or CO_2 mixtures result in overall total-to-total efficiencies in excess of 92.5%; where the highest turbine efficiency is achieved for the turbine operating with pure CO_2, whilst this reduces by a maximum of 1.1 percentage points for the $CO_2/TiCL_4$ mixture. This reduction in efficiency is because the $CO_2/TiCL_4$ turbine is limited to a maximum of six design stages in order to meet the imposed mechanical design criteria, whilst the pure CO_2 turbine can accommodate thirteen stages leading to higher aerodynamic efficiency. The difference between the two cases is the result of a higher mass-flow rate for the $CO_2/TiCL_4$ mixture (66% greater than for pure CO_2), which results in high rotor bending stresses and limits the number of stages to comply with the design criteria. It is also found that designing the turbine at loading and flow coefficients of 0.8 and 0.6 respectively, whilst fixing the degree of reaction and pitch-to-chord ratio to values of 0.5 and 0.85 respectively, resulted in an efficiency enhancement of 0.2% with respect to a baseline design produced at loading and flow coefficients of 1.0 and 0.5. This increase is due to being able to increase the number of stages from eleven to fifteen. This indicates that there is not much benefit in modifying key design parameters to improve the turbine efficiency as the 0.2% efficiency enhancement is considered within the margin of accuracy of mean-line flow path design.

Keywords: Axial turbine, mean-line design, CO_2 mixtures, flow path design, pure CO_2.

1. INTRODUCTION

Mixing CO_2 with certain additives, namely $CO_2/TiCl_4$, CO_2/C_6F_6 and CO_2/SO_2, has been shown to increase the critical temperature of the working fluid compared to the pure CO_2. This enables an economically feasible condensation at elevated air temperatures in dry regions where CSP plants are located and thus significantly reducing compression work. Therefore, the utilisation of certain CO_2 mixtures has been found to be promising for CSP applications achieving up to six percentage points increase in cycle efficiency compared to a simple recuperated non-condensing CO_2 cycle, depending on the implemented cycle configuration and the nature of the selected mixture [1]. Using CO_2 mixtures has the potential to reduce the capital expenditure (CAPEX) by 30% and operational expenditures (OPEX) by 35% compared to state-of-the-art steam cycles [2]. Therefore, the SCARABEUS project aims to demonstrate the potential of using CO_2 mixtures for large-scale plants in the order of 100 MW_e.

To achieve this aim, multiple dopants have been identified to increase the critical temperature of CO_2 based working fluids. Morosini et al. [3] and Manzolini et al. [4] examined the potential of using CO_2/C_6F_6 mixture for a power cycle coupled

with a solar power tower system. A simple recuperated cycle efficiency of 42.5% and 46.5% has been obtained by operating at maximum cycle temperatures of 550 and 650 °C respectively. The same mixture has been further examined by Rodriguez et al. [5] in addition to considering two other mixtures ($CO_2/TiCl_4$ and CO_2/SO_2) with respect to a pure CO_2 for simple recuperated cycle configurations. As a result, CO_2 mixtures achieved thermal efficiency up to 51.6% at a maximum cycle temperature of 700°C. Therefore, the selected mixtures have shown to outperform both steam Rankine and pure sCO_2 cycles. Later, Morosini et al. [6] examined the performance of multiple cycles operating with CO_2/SO_2 mixture. The results of the analysis showed that the recompression layout results in a power block electric efficiency of 48.67% (2.33% higher than the respective sCO_2 cycle).

Similarly, Crespi et al. [7] examined the cycle performance operating with the $CO_2/TiCl_4$ and CO_2/C_6F_6 mixtures for recuperated and precompression cycle configurations respectively. Using the mixtures resulted in an efficiency gain of 4-5% points with respect to an equivalent cycle operating with pure CO_2. Furthermore, Crespi et al. [1] investigated the potential of introducing CO_2/SO_2 in a transcritical recompression cycle. This resulted in promising results where cycles thermal efficiencies of $\approx$ 45% and greater than 51% have been obtained at 550 and 700 °C respectively. Thus, the CO_2/SO_2 mixture has shown an efficiency equal to or higher than the other promising mixtures including $CO_2/TiCl_4$ and CO_2/C_6F_6.

Ultimately, for the SCARABEUS project, three candidate mixtures have been found to be promising for CO_2 power cycles including $CO_2/TiCl_4$, CO_2/C_6F_6 and CO_2/SO_2. The thermal stability of these candidate mixtures has been previously investigated within the project consortium and only C_6F_6 showed signs of thermal degradation at temperatures greater than 600°C [8]. Apart from thermal stability concerns, the use of the $TiCL_4$ dopant may face some potential limitations due to possible corrosion effects resulting from the high reactivity of $TiCL_4$ with air moisture. Additionally, the formation of H_2SO_4 when SO_2 combines with water may add some challenges to the use of the SO_2 dopant. Nonetheless, it is worth mentioning that the health hazards associated with both SO_2 and $TiCl_4$ are very similar to hazards associated with other fluids that are commonly employed in CSP plants, such as Therminol VP1 [1]. As for the environmental hazards, none of the selected mixtures have any significant global warming potential or ozone depletion potential. Therefore, the environmental impact of the selected dopants is considered minimal.

Given that the previous studies showed that the best cycle configuration is strongly dependent on the dopant [7], simple recuperated, precompression and recompression cycles have been selected for $CO_2/TiCl_4$, CO_2/C_6F_6 and CO_2/SO_2 respectively [9]. Considering that the main target of the SCARABEUS project is to reduce the cost of the power block, Morosini et al. [6] carried out an economic analysis for the power block of a transcritical cycle operating with recompression CO_2/SO_2 cycle. A specific CAPEX of 1000 \$/kW$_e$ was obtained for the cycle compared to 1160 \$/kW$_e$ for the sCO_2 cycle with the same cycle layout. Likewise, the CAPEX of a simple recuperated cycle working with the optimal CO_2/SO_2 mixture was found to be 718 \$/kW$_e$ compared to a CAPEX of 795 \$/kW$_e$ for the same cycle layout operating with pure CO_2.

Bearing in mind that the cycle performance is greatly dependent upon the performance of the different cycle components, particularly the turbine and heat-exchangers, some of the recent research focused on designing sCO_2 turbines for different scales. Enhancing the design and performance of the different cycle components should result in better system performance and hence, cost reduction for the overall CSP technology. To realise this development, a multi-stage turbine design process needs to be carried out starting from the preliminary aerodynamic design and optimisation, using a combination of one-dimensional mean-line design and suitable loss models and ending with through-flow analysis and computational fluid dynamic (CFD) analysis. Ultimately, the design should be validated against experimental data to give credence to the developed model.

In regards to the preliminary aerodynamic design stage, some studies presented the sCO_2 turbine design for small-scale applications. Qi et al. [10] presented a mean-line design for a 100-200 kW sCO_2 radial turbine; where several designs have been developed for a set of loading and flow coefficients to allow for selecting feasible designs according to the manufacturing and structural constraints. Holaind et al. [11] addressed the design of a small-scale sCO_2 radial turbine with output power ranging from 50-85 kW. Furthermore, Zhou et al. [12] proposed a 1.5 MW sCO_2 radial inflow turbine design and the 1D results were shown to be consistent results with 3D CFD simulation results with a maximum deviation of 5%. LV et al. [13] presented an optimisation study for the performance of a radial inflow turbine using sCO_2 working fluid. This was done by combining a one-dimensional design method with an optimisation algorithm for both nominal and off-design performance conditions. The overall total-to-static efficiency showed a good agreement between the 1D model and the CFD results. Saeed et al. [14] designed a sCO_2 radial turbine within the analysis process of a 10 MW$_e$ recompression supercritical carbon dioxide cycle. The turbine design and optimisation models were validated against CFD simulations. The validation results for the design and optimisation models showed a maximum difference of six percent in the turbine mass flow rate which was considered to be within the acceptable error range.

Radial turbines are known to be suitable for small-scale applications and hence, the previous studies focused on designing radial turbines producing power of up to 10 MW. Nonetheless, axial turbines are capable of handling high mass flow rates more efficiently than radial turbines and hence are suitable for large-scale applications; including electrical power generation and propulsion systems. To advance the state of the art with regards to sCO_2 axial turbine design, Schmitt et al. [15] presented the preliminary aerodynamic design of a first stage of a 100 MW sCO_2 turbine. Moroz et al. [16] studied some design aspects of a 100 MW sCO_2 turbine. The study included the integration of aerodynamic-structural optimisation with the mean-line design to maximise the turbine efficiency along with satisfying the structural limitations. Zhang et al. [17] proposed a design for sCO_2 axial turbine for an output power of 15 MW. The one-dimensional design was validated against CFD simulations and a good agreement was obtained between both results. Finally, Shi et al. [18] presented

a three-stage 10 MW sCO_2 axial turbine design using 3D CFD simulations, optimisation methods and off-design performance analysis.

Several test rigs were developed with a power rating of up to 8 MW to examine the feasibility and operation of CO_2 cycles. The majority of the present test rigs considered radial turbine configurations with only a single 1 MW axial turbine [19–24]. Additionally, some conceptual designs have been presented for large-scale turbines with power ratings of 246 MW, 450 MW, and 645 MW and turbine efficiencies of 92.9%, 90% and 90% have been predicted respectively [25–27].

Most of the sCO_2 turbomachinery designs and test facilities presented in the literature review have considered small-scale radial turbines with fewer studies focused on developing the designs for large-scale axial turbines of around 100 MW power rating. The earlier studies and conceptual designs have focused on aspects of turbine designs for sCO_2 based plants without accounting for the effects of introducing CO_2 mixtures. Comparatively, the SCARABEUS project is concerned with the application of CO_2 mixtures for large-scale CSP plants (100 MW_e). Some aspects of large-scale axial turbine design operating with CO_2 mixtures has been presented in the authors previous work [9]. This work included the design of multiple flow paths operating with $CO_2/TiCl_4$, CO_2/C_6F_6 and CO_2/SO_2 mixtures in addition to investigating the sensitivity of the design to changing the cycle boundary conditions and molar fraction of these mixtures. Ultimately, it was shown that using CO_2 mixtures resulted in a total-to-total turbine efficiency in excess of 92%.

The differences in the flow path design resulting from the use of CO_2 mixtures with respect to the pure CO_2 have not been discussed within the earlier analysis conducted by the authors. Therefore, it is important to explore if any differences are imposed by introducing CO_2 mixtures compared to pure CO_2, and to also highlight if there is any impact of using the mixtures on the turbine performance compared to the pure CO_2. Thus, this study aims to investigate the differences in turbine flow path designs operating with pure CO_2 compared to CO_2 mixtures, whilst taking into account aerodynamic, rotordynamic and mechanical design aspects which are assessed using a mean-line design process. The aim of this study also extends to exploring whether there is any advantage in modifying key design parameters to further improve the efficiency of the turbine. This includes examining the effect of changing the loading coefficient, flow coefficient, degree of reaction and pitch-to-chord ratio on the flow path design and overall turbine performance.

2. DESIGN METHODOLOGY

An in-house mean-line design tool is used to design the turbine, which assumes a constant hub diameter [9, 28, 29]. Within the current research framework, the flow paths are designed at a constant hub diameter to avoid the potential rotordynamic and mechanical challenges associated with turbines designed at a constant mean-diameter. Designing the flow path at a constant mean-diameter results in a hub diameter that is decreasing from inlet to exhaust and hence, results in an increased radius ratio along the turbine. On this matter, larger chord sizes are needed to limit the stresses on the blade roots for the increased radius ratio; where larger chord sizes result in larger roots and add additional challenges for the stiffness and rotordyanmics of the rotor.

The turbine design process is initiated by defining the boundary conditions; the total inlet temperature, the total inlet pressure, the pressure ratio, the mass flow rate and the inlet flow angle. This is followed by defining some of the commonly used dimensionless parameters such as the loading coefficient, flow coefficient, degree of reaction and pitch-to-chord ratio [9, 29]. Repeating turbine stages are assumed within the design methodology where the blade geometry, velocity triangles and thermodynamic properties are obtained for the given set of inputs. Ultimately, the design tool is integrated with the Aungier loss model [30] to predict the performance of the turbine accounting for profile, secondary, tip clearance, trailing edge, shock and supersonic losses. The turbine aerodynamic performance is represented using the total-to-total turbine efficiency which is defined in Equation 1:

$$\eta_{tt} = \left[1 + \left(\frac{\zeta_R w_3^3 + \zeta_S C_2^2 \frac{T_3}{T_2}}{2(h_{01} - h_{03})}\right)\right]^{-1} \tag{1}$$

where C and w are the absolute and relative velocities and ζ_S and ζ_R are the enthalpy loss coefficients for the stator and rotor respectively, $(h_{01} - h_{03})$ is the total enthalpy drop across the turbine stage.

The aerodynamic losses are introduced within the mean-line design model in the form of stagnation pressure coefficients for the stator and rotor (Y_S and Y_R) which are predicted using the Aungier loss model [30]. To estimate the turbine total-to-total efficiency, using Equation 1, the pressure loss coefficients can be converted to enthalpy loss coefficients using the following expressions [31]:

$$\zeta_R = Y_R \times \left(1 + 0.5(k\ {M_3}^2)\right) \tag{2}$$

$$\zeta_S = Y_S \times \left(1 + 0.5(k\ {M_2}^2)\right) \tag{3}$$

where k is the specific heat ratio, and M_2 and M_3 are the absolute rotor inlet and relative rotor outlet Mach numbers respectively.

Considering that the expanding fluids (CO_2 and CO_2 mixtures) are characterised with a high power density, the bending stresses generated by the fluid expansion are more critical than the centrifugal stresses generated by blade rotation. Therefore, further to considering the aerodynamic performance, rotodynamic and mechanical design constraints have been specified within the mean-line design methodology based on industrial experience. In brief, the constraints were set to limit the rotor bending stresses, slenderness ratio (the ratio of the bearing span with respect to the hub diameter) and chord length to 130 MPa, 9 and 100 mm respectively. The flow paths are designed in this study using a manual process that involves tuning and adjusting the number of stages and the number of blades to meet the set design criteria. This ensures that multiple flow paths with high aerodynamic performance can be achieved that comply with the specified mechanical and rotordynamic design criteria. The flow paths are designed to operate at a synchronous rotational speed of 3,000 RPM for the net CSP plant power of 100 MW, assuming a connection to a 50 Hz grid. This is due to the difficulty of incorporating a

gearbox for such turbine scales, which means non-synchronous designs are not suitable. Further details about the design criteria can be found in the authors previous work [9].

It is worth mentioning that the mean-line design tool has been verified against multiple cases from the literature operating with different working fluids including air, sCO_2 and R1233zd(E). A maximum percentage difference of 1.3% and 1.2% in the total-to-total and total-to-static efficiency, respectively, was obtained between the developed model and the verification cases. The full verification results are presented in the authors previous works [9, 29]. Furthermore, the mean-line design tool has been verified against CFD simulation results for a 130 MW axial turbine operating with $80\%CO_2/20\%SO_2$ mixture. A good agreement was obtained between the mean-line model and CFD results where a maximum difference in the mass flow rate and total-to-total efficiency of 0.5% and 1.0% was achieved respectively [32]. For the same turbine design, the blade has also been evaluated using finite element analysis to ensure mechanical stresses are within the specified limits (i.e., the maximum stress is less than 260 MPa). This analysis included adjusting the fillet at the base of the blade to satisfy the stress constraints. Ultimately, this demonstrates that using the bending stress limit applied within the mean-line design model results in feasible turbine geometries from a mechanical design perspective. Further improvements to the 3D blade geometry can be achieved using blade shape optimisation to match the cycle operating conditions alongside improving the turbine performance [32]; however, such analysis is beyond the scope of the present study.

Given that the current study deals with modelling both pure CO_2 and CO_2 mixtures, the thermodynamic properties of the candidate mixtures are obtained using the Peng-Robinson equation of state (EoS). Binary interaction parameters (k_{ij}) were used to tune the mixing model to predict the vapour-liquid equilibrium properties of the examined mixtures accurately. The parameters have been obtained by regression of experimental VLE (Vapour Liquid Equilibrium) data available within the Aspen library [33–35].

3. RESULTS AND DISCUSSION

In the current study, multiple flow paths are designed for a large-scale axial turbine operating with $CO_2/TiCL_4$, CO_2 $/C_6F_6$ and CO_2 $/SO_2$ mixtures alongside pure CO_2. Using the in-house design tool, the flow path designs are optimised for aerodynamic performance considering both the rotordynamic and mechanical design constraints. Initially, the number of design stages is assumed and hence, the flow path is designed and its aerodynamic performance is evaluated. The flow paths are designed at a fixed loading coefficient, flow coefficient, degree of reaction, pitch-to-chord ratio and trailing edge-to-throat ratio of 1.0, 0.5, 0.5, 0.85 and 0.05 respectively.

In a previous analysis done by the authors [9], it has been found that increasing the number of stages results in higher turbine efficiency. Increasing the number of stages results in a reduction in the peripheral speed which is dictated by the design methodology where a fixed loading coefficient is assumed at a constant rotational speed. Therefore, smaller hub diameters are obtained at reduced peripheral speeds, which results in enhanced turbine performance. The reduction in peripheral speeds results in designs with longer blade heights, and hence a reduced chord-to-height ratio and reduced secondary flow losses. Additionally, lower tip clearance losses are experienced with small hub diameters since the clearance gap is defined as a fixed percentage of the tip diameter. Therefore, increasing the number of stages results in a smaller hub diameter and high aerodynamic performance. More specifically, up to 5% enhancement in the total-to-total efficiency was obtained when increasing the number of stages from four to fourteen for the $CO_2/TiCL_4$ and CO_2 $/SO_2$ mixtures.

The flow path designs are explained in the following subsections using the same methodology; where the efficiency is optimised by reducing the hub diameter alongside complying with the specified mechanical and rotodynamic design constraints. Given that the optimum cycle configuration has been found to change with the selected mixture, recuperated (Figure 1), precompression (Figure 2) and recompression cycles (Figure 3) were found to be optimum for the $CO_2/TiCL_4$, CO_2/C_6F_6 and CO_2 $/SO_2$ mixtures [9] respectively. A recuperated cycle is composed of a recuperator (R), pump, primary cooler (PC), primary heat exchanger (PHX), and turbine (T). Recompression and precompression cycles are proposed to enhance the performance of the recuperated cycle. The recompression cycle involves splitting the internal heat recovery process among the low and high-temperature recuperators to balance the heat capacity rates of the two streams and reduce cycle irreversibilities. In comparison, the precompression cycle involves the placement of an additional compressor between the low and high-temperature recuperators to overcome the constraint imposed by the condensation temperature on the exhaust pressure in recuperated cycles, and hence increase the specific work of the cycle.

It is worth mentioning that the performance of precompression and recompression cycles will depend on the efficiency of the compressor in addition to the turbine. In this analysis, the optimal cycles were identified under the assumption of fixed isentropic efficiencies for all rotating machinery, and the focus is on the turbine. However, the design of a suitable compressor for these novel working fluids is another critical task, and this should be considered in future work.

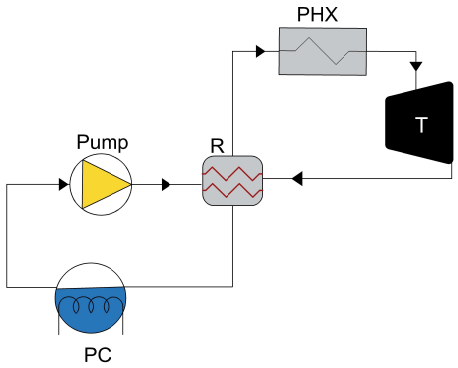

FIGURE 1: SIMPLE RECUPERATED CYCLE WITH A RECUPERATOR (R), PUMP, PRIMARY COOLER (PC), PRIMARY HEAT EXCHANGER (PHX), AND TURBINE (T) OPERATING WITH THE $CO_2/TICL_4$ MIXTURE [9].

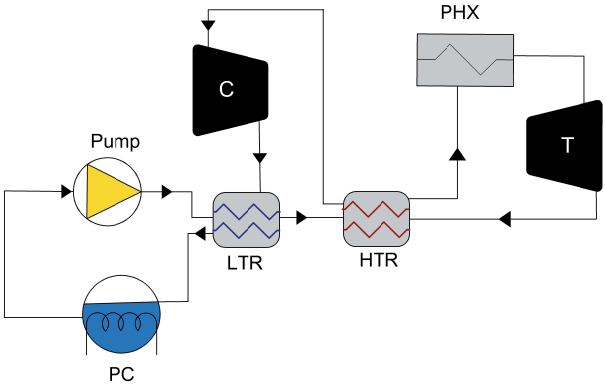

FIGURE 2: PRECOMPRESSION CYCLE WITH A HIGH-TEMPERATURE RECUPERATOR (HTR), LOW-TEMPERATURE RECUPERATOR (LTR), PUMP, COMPRESSOR (C), PC, PHX AND T OPERATING WITH THE CO_2/C_6F_6 MIXTURE [9].

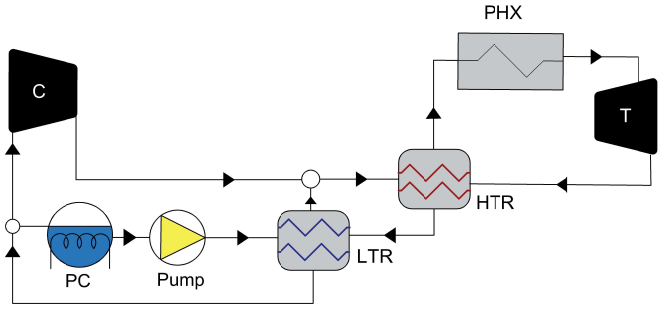

FIGURE 3: RECOMPRESSION WITH A HTR, LTR, PUMP, C, PC, PHX AND T OPERATING WITH THE CO_2/SO_2 MIXTURE [9].

TABLE 1: OPERATING CONDITIONS FOR CO_2 MIXTURES OPERATING WITH DIFFERENT CYCLE CONFIGURATIONS [9].

Fluid	CO_2/ $TiCL_4$	CO_2/ C_6F_6	CO_2/SO_2
$\dot{m}$ [kg/s]	1241	877	827
T_{01}[K]		973	
P_{01}[MPa]	24.3	23.9	23.9
P_{03}[MPa]	9.7	5.63	8.15
X_i[%]	17	14.5	20
W[MW]	128.9	151.5	141.35

The flow paths are firstly designed for the optimised cycle configurations and molar fractions at a total inlet temperature of 973 K. The boundary conditions for the CO_2 mixtures are obtained based on the cycle analysis conducted in Salah et al. [9] and are summarised in Table 1. The optimum molar fractions were found to be 17, 14.5 and 30% for the $CO_2/TiCL_4$, CO_2/C_6F_6 and CO_2 /SO_2, respectively, resulting in thermal cycle efficiencies of 51.5, 50.5 and 51.5% for the three mixtures [9]. Meanwhile, in this analysis, the CO_2/SO_2 mixture is considered with a molar fraction of 20% for reduced environmental hazards.

Figure 4 shows the total-to-total efficiency (η_{tt}) and the number of stages of the flow paths designed for different cycle configurations as presented in an earlier analysis by the authors [9]. It was found that using the $CO_2/TiCl_4$ mixture resulted in the shortest flow-path length compared to both CO_2/C_6F_6 and CO_2/SO_2. Furthermore, the three CO_2 mixtures resulted in an overall total-to-total flow path efficiency above 93% at a turbine inlet temperature of 973K. According to the turbine boundary conditions dictated by the cycle analysis, different turbine designs and number of stages are obtained for all mixtures. Eight stages are obtained for the $CO_2/TiCl_4$ to produce a power of 129 MW at a pressure ratio of 2.5. Whereas fifteen and sixteen design stages are required to produce power of 151.5 and 141.5 MW at pressure ratios of 4.2 and 2.9 for the CO_2/C_6F_6 and CO_2/SO_2 respectively. This is due to the significant increase in the mass-flow rate required for the $CO_2/TiCl_4$ mixture for a constant power output of the plant (100 MW_e). The $CO_2/TiCl_4$ has the least specific work followed by the CO_2/C_6F_6 and CO_2/SO_2. Thus, a mass flow rate of 1241 kg/s is required for the recuperated cycle with respect to 877 and 827 for the precompression and recompression cycles respectively. This results in higher bending stresses applied on the rotor blades and hence, in the least number of stages obtained for the $CO_2/TiCl_4$. Accordingly, flow path efficiencies of 93.3, 93.8 and 94.0% are obtained for the $CO_2/TiCl_4$, CO_2/C_6F_6 and CO_2/SO_2 respectively [9].

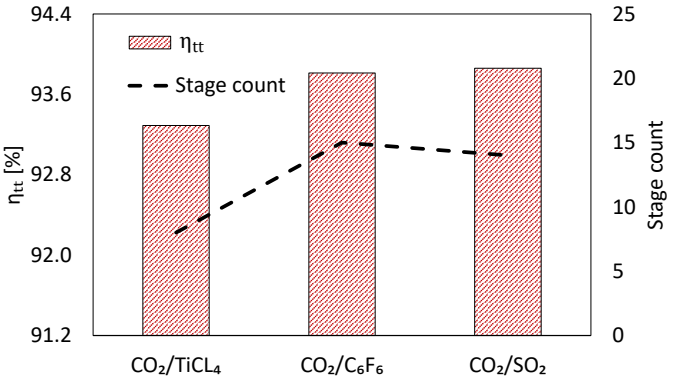

FIGURE 4: STAGE COUNT AND TOTAL-TO-TOTAL EFFICIENCY (η_{tt}) FOR THE THREE MIXTURES OPERATING WITH DIFFERENT CYCLE CONFIGURATIONS [9].

To have a fair comparison between the effect of the three-candidate mixtures on the flow path design with respect to the pure CO_2, recuperated cycle configurations are selected for all working fluids where the same power output is assumed for all designs. This is to overcome the differences in the turbine boundary conditions imposed by operating with precompression and recompression cycle configurations for the CO_2/C_6F_6 and CO_2/SO_2 mixtures. The results of this analysis are discussed in Section 3.1. Furthermore, the comparison of the flow path designs was extended to address the axial turbine differences in the design dictated by the fluid properties by decoupling the turbine design from the cycle conditions. To achieve this aim, the flow paths are designed at a fixed volumetric flow rate and volumetric expansion ratio (Section 3.1.1). Ultimately, the effects of changing the design variables on the flow path design are presented in Section 3.2.

3.1 Flow path comparison for fixed cycle configurations

Flow path designs are explained in this section for the three mixtures and the pure CO_2 at the boundary conditions summarised in Table 2 [36]. The boundary conditions for the CO_2 mixtures and pure CO_2 are obtained based on the cycle analysis conducted by Aqel et al. [36] and Manzolini et al. [37] respectively.

TABLE 2: OPERATING CONDITIONS FOR PURE SCO_2 AND CO_2 MIXTURES OPERATING WITH RECUPERATED CYCLES.

Fluid	CO_2	CO_2/$TiCL_4$	CO_2/C_6F_6	CO_2/SO_2
$\dot{m}$ [kg/s]	909	1393	1054	738
T_{01}[K]			973	
P_{01}[MPa]			25	
P_{03}[MPa]	10.5	10.1	7.7	7.4
X_i[%]	-	17.4	15.7	26.4
W[MW]	140	141	141	137

The flow paths design details for the 1st and last turbine stages are summarised in Table 3. It is evident from the presented results that pure CO_2 and CO_2 mixtures, operating with recuperative cycles, result in flow path designs with efficiency in excess of 92.5%. Though similar performance is predicted for all working fluids, there exist some differences between the flow path designs of the CO_2 mixtures with respect to the pure CO_2.

The CO_2/SO_2 resulted in the longest flow path design while CO_2/$TiCL_4$ resulted in the shortest flow path with the least number of stages due to experiencing the highest bending stresses. This is due to the thermo-physical properties of CO_2/$TiCL_4$ where the smallest specific work is obtained for the CO_2/$TiCL_4$ compared to the other working fluids. Therefore, a higher mass flow rate is needed to produce the same turbine power; 89% mass flow rate higher than the CO_2/SO_2 case. Hence, larger bending stress is applied to the rotor blades. Sixteen design stages are required for the CO_2/SO_2 compared to thirteen, twelve and seven stages for pure CO_2, CO_2/C_6F_6 and CO_2/$TiCL_4$ respectively.

It can be noticed that the designs of CO_2/C_6F_6, CO_2/SO_2 and pure CO_2 are very similar with regards to the hub diameter (approximately 600 mm as shown in Figure 5) and chord length with the shortest chord length is obtained by the CO_2/SO_2 flow path. On the other hand, due to the high stresses experienced in CO_2/$TiCL_4$, a shorter flow path length and hence a larger hub diameter of 686 mm are obtained. Additionally, the highest aspect ratio is experienced in the last stage of CO_2/SO_2 flow path followed by pure CO_2, CO_2/C_6F_6 and CO_2/SO_2.

Regarding the turbine performance, unlike the cycle analysis, where up to 6% enhancement is achieved by operating with precompression and recompression cycles compared to a simple recuperated CO_2 cycle, a lower turbine efficiency is obtained by using CO_2 mixtures compared to the pure CO_2 case; where a maximum and minimum efficiency reduction of 1% and 0.2% are achieved for the CO_2/$TiCL_4$ and CO_2/C_6F_6 respectively.

Contrary to the results obtained by operating with precompression and recompression cycles, designing the turbine flow paths within recuperated cycles resulted in different flow path designs for the CO_2/C_6F_6 and CO_2/SO_2; where the CO_2/C_6F_6 flow path is associated with less number of stages compared to the CO_2/SO_2 (12 versus 16 stages). For recuperated cycles with the same power output, a greater mass flow rate is required for CO_2/C_6F_6, 1054 compared to 877 kg/s in the precompression cycle, based on the specific work obtained using the imposed boundary conditions. Hence, operating within a recuperated cycle results in higher bending stress and the number of stages is reduced for the CO_2/C_6F_6 from fifteen, for the precompression cycle (Figure 4), to twelve stages to comply with the mechanical and rotodynamic design criteria.

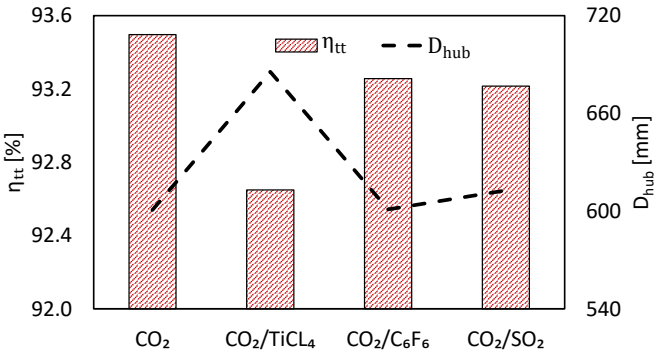

FIGURE 5: HUB DIAMETER (D_{hub}) AND TOTAL-TO-TOTAL EFFICIENCY (η_{tt}) FOR THE THREE MIXTURES OPERATING WITH RECUPERATED CYCLES.

3.1.1 Flow path comparison at fixed volumetric flow rate and expansion ratio. This section aims to explore if any differences in the design are introduced due to differences in the thermo-physical properties of the working fluids. To do this, the cycle and turbine are decoupled and the flow paths are designed at a fixed volumetric flow rate and volumetric expansion ratio; where the mass flow rate and outlet pressure for each mixture are set to allow for a constant volumetric flow rate ($\dot{V}$) and expansion ratio (VR) of 9.4 m^3/s and 0.49, respectively, for all designs. The volumetric flow rate and expansion ratio are obtained at the average fluid density and specific heat ratio between the inlet and outlet conditions. Finally, an inlet pressure of 25 MPa and a molar fraction of 20% have been set for all working fluids. A summary of the turbine boundary conditions is presented in Table 4.

For a volumetric flow rate and expansion ratio of 9.4 m^3/s and 0.49, respectively, thirteen and twelve turbine stages are obtained for the CO_2/SO_2 and pure CO_2 compared to six stages for the CO_2/C_6F_6 and CO_2/$TiCL_4$ mixtures. Therefore, the CO_2/SO_2 design showed a similar hub diameter to the pure CO_2, of approximately 600 mm (Figure 6), with a similar total-total efficiency of 93.9%. This is due to the similar density and specific heat ratio for the CO_2/SO_2 mixture at 20% molar fraction with respect to the pure CO_2. This results in similar mass flow rates, for the same volumetric flow rate and expansion ratio, and hence, similar number of stages are assigned for both designs (12 and 13). These design details are summarised in Table 5.

On the contrary, the CO_2/C_6F_6 results in the lowest total-to-total efficiency with respect to the pure CO_2 case; this is mainly due to designing the flow path with approximately half the number

TABLE 3: FLOW PATH DESIGN DETAILS FOR PURE CO_2 TURBINE COMPARED TO CO_2 MIXTURES OPERATING WITH RECUPERATED CYCLES.

Parameter	Pure CO_2		$CO_2/TiCl_4$		CO_2/C_6F_6		CO_2/SO_2	
	1st stage	last stage	1st stage	last stage	1st stage	last stage	1st stage	last stage
Number of stages [-]	13		7		12		16	
Hub diameter [mm]	601		686		601		613	
Number of rotor blades	46	39	44	37	46	36	59	45
Radial tip clearance [mm]	0.52	0.59	0.56	0.62	0.50	0.60	0.50	0.60
Rotor chord length [mm]	54	69	62	79	53	76	42	61
Rotor blade height [mm]	67	118	55	99	54	123	49	113
Diffusion angle [°]	2.0	3.3	2.9	4.8	2.6	5.0	2.2	4.4
Staggering angle [°]	35	36	35	36	35	37	35	36
Aspect ratio [-]	1.24	1.71	0.88	1.24	1.03	1.63	1.19	1.87
Total-to-total efficiency [%]	93.50		92.65		93.26		93.22	

TABLE 4: OPERATING CONDITIONS OF PURE CO_2 AND CO_2 MIXTURES AT A CONSTANT VR AND $\dot{V}$.

Fluid	CO_2	$CO_2/TiCL_4$	CO_2/C_6F_6	CO_2/SO_2
$\dot{m}$ [kg/s]	909	1514	1479	995
T_{01}[K]	973			
P_{01}[MPa]	25			
P_{03}[MPa]	10.5	10.1	7.7	7.4
X_i[%]	-		20	
γ [-]	1.212	1.197	1.23	1.22
ρ $[kg/m^3]$	96.4	160.7	160.0	105.6

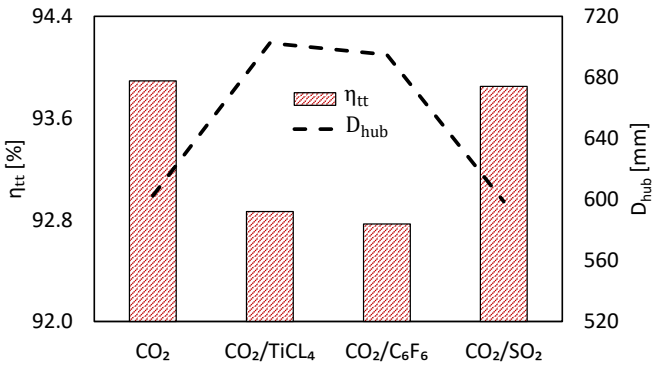

FIGURE 6: HUB DIAMETER (D_{hub}) AND TOTAL-TO-TOTAL EFFICIENCY (η_{tt}) FOR THE THREE MIXTURES AT A FIXED VOLUMETRIC EXPANSION RATIO AND FLOW RATE.

of stages of the pure CO_2 flow path which results in a larger hub diameter of approximately 700 mm. For the CO_2/C_6F_6 mixture, a greater mass flow rate is needed compared to the pure CO_2 (in excess of 62%) to operate at the same volumetric flow rate and ratio. This results in much higher bending stresses acting on the rotor blades, and hence less stages are required to comply with the mechanical and rotor-dyanmic design criteria. Similar conclusions can be retrieved for the $CO_2/TiCL_4$ case which has a similar density with respect to the CO_2/C_6F_6. Therefore, similar turbine designs are obtained for both CO_2/C_6F_6 and $CO_2/TiCL_4$ mixtures.

Ultimately, designing the turbine to operate within different cycle configurations results in similar flow path designs for both CO_2/C_6F_6 and CO_2/SO_2 mixtures. Whilst, designing the turbine to operate within fixed cycle configurations (recuperated) results in different designs for both mixtures and similar designs between the CO_2/C_6F_6 and pure CO_2. Decoupling the cycle conditions results in significant differences between the flow path designs of both CO_2/C_6F_6 and CO_2/SO_2 mixtures and similar flow path designs for the CO_2/SO_2 and pure CO_2. It can be noted that regardless of the cycle configuration, for all design cases, the $CO_2/TiCL_4$ mixture results in designs with the shortest flow path length (with 6 to 8 design stages).

3.2 Parametric study results

In view of the fact that the previous flow paths were designed at fixed design parameters, further analysis has been conducted to investigate the effect of aerodynamic design variables such as the flow coefficient (ϕ), loading coefficient (ψ), degree of reaction (λ) and pitch-to-chord ratio (s/c) on the performance of axial turbines operating with CO_2 mixtures.

To proceed further with the analysis, the CO_2/C_6F_6 flow path was selected according to the health and environmental considerations discussed in Section 1. Bearing in mind that the CO_2/C_6F_6 mixture showed some signs of thermal instability at temperatures above 600°C, a precompression cycle with a maximum temperature of 550°C (823 K) is found to be the most thermally stable [38]. Consequently, a parametric study is presented in this section to investigate the effect of the design variables on the performance and flow path design of CO_2/C_6F_6 mixture operating within a precompression cycle. The aim of this section is to explore whether there is any advantage in further modifying the design parameters with the goal of further improving the efficiency of the turbine. A summary of the boundary conditions for the CO_2/C_6F_6 flow path is shown in Table 6.

The velocity triangles and meridional view of the CO_2/C_6F_6 flow path design are shown in Figures 7 & 8. These results are obtained at the baseline design point operating at a loading coefficient, flow coefficient, degree of reaction and pitch-to-chord ratio of 1.0, 0.5, 0.5 and 0.85 respectively. Eleven turbine stages are required for the CO_2/C_6F_6 with a hub diameter of 630 mm as shown in Figure 7; where the unfilled and filled shapes represent the stator and rotor respectively.

TABLE 5: FLOW PATH DESIGN DETAILS FOR PURE CO_2 TURBINE COMPARED TO CO_2 MIXTURES AT CONSTANT VR AND $\dot{V}$.

Parameter	Pure CO_2		$CO_2/TiCl_4$		CO_2/C_6F_6		CO_2/SO_2	
	1^{st} stage	last stage	1^{st} stage	last stage	1^{st} stage	last stage	1^{st} stage	last stage
Number of stages [-]	13		6		6		12	
Hub diameter [m]	602		702		695		599	
Number of rotor blades	46	39	44	37	43	37	41	36
Radial tip clearance [mm]	0.52	0.59	0.57	0.63	0.57	0.62	0.51	0.59
Rotor chord length [mm]	54	69	64	80	65	80	60	75
Rotor blade height [mm]	67	118	55	94	56	94	68	119
Diffusion angle [°]	2.0	3.3	3.1	4.9	3.1	4.8	1.9	3.3
Staggering angle [°]	35	36	35	36	35	36	35	36
Aspect ratio [-]	1.23	1.70	0.86	1.16	0.86	1.18	1.12	1.59
Total-to-total efficiency [%]	93.89		92.86		92.77		93.85	

TABLE 6: OPERATING CONDITIONS FOR THE CO_2/C_6F_6 MIXTURE AT 823 K.

Parameter	Unite	CO_2/C_6F_6
Inlet Temperature [T_{01}]	K	823
Inlet Pressure [P_{01}]	MPa	23.9
Outlet pressure [P_{03}]	MPa	6.1
Mass flow rate [$\dot{m}$]	kg/s	1152
Optimum molar fraction X_i	%	14.5

TABLE 7: FLOW PATH DESIGN DETAILS FOR THE CO_2/C_6F_6 MIXTURE.

Parameter	CO_2/C_6F_6	
	1^{st} stage	last stage
Molar fraction [%]	14.5	
Number of stages [-]	11	
Hub diameter [m]	630	
Number of rotor blades	47	35
Radial tip clearance [mm]	0.51	0.63
Rotor chord length [mm]	53.7	81.9
Rotor blade height [mm]	50.7	130.3
Diffusion angle [°]	2.9	6.3
Staggering angle [°]	35	37
Aspect ratio [-]	0.95	1.60
Total-to-total efficiency [%]	93.68	

The CO_2/C_6F_6 enter the stator blade row at a zero incidence angle with $\alpha_1 = 0$ where it expands and hence, speeds up in the stator blades till reaching an absolute flow velocity of 120 m/s and exits at an absolute angle $\alpha_2 = 64.8°$. Then the fluid enters the rotor blades with the same velocity and continues to expand in the rotor blades with a specified degree of reaction of 0.5. As a result, the working fluid leaves the rotor blades with a relative flow angle of $\beta_3 = 64.9°$ and a relative flow velocity $w_3 = 53.5\ m/s$.

The turbine design has an inlet stator annulus area of 0.10 m^2 and an outlet annulus area of 0.30 m^2 and stator inlet blade height of 48.3 mm and a rotor outlet blade height of 130 mm. As a consequence of the increased blade heights at the last turbine stage, higher bending stresses are experienced with the later design stages in comparison with the earlier stages. It is worth mentioning that all the flow path designs presented in the current study have similar velocity triangles to the CO_2/C_6F_6 mixture (Figure 8) due to designing them at a constant loading coefficient, flow coefficient and degree of reaction of 1.0, 0.5 and 0.5 respectively.

Within this section, the effect of changing these design parameters on the aerodynamic turbine performance and flow path design was investigated considering constrained (CD) and non-constrained (NCD) design criteria. This is to highlight the effect of changing those parameters from a purely aerodynamic standpoint compared to considering both rotordynamic and mechanical design considerations throughout the design process.

For the non-constrained criteria, the turbine aerodynamic performance is investigated for a given number of stages and number of rotor blades, over a wide range of design variables, and the constraints imposed on the rotoric bending stress and slenderness ratio are removed. Whilst, in the constrained criteria, new turbines are designed over a range of design variables ϕ, ψ, Λ, s/c considering the rotordynamic and mechanical design criteria. This means that for the non-contained criteria, the aerodynamic performance is investigated for a fixed design (with a fixed number of stages and rotor blades) at variable design parameters. However, different turbine flow paths with different numbers of stages and blades are designed for the constrained design criteria.

Figures 9 - 12 show the parametric analysis results of the CO_2/C_6F_6 flow path; where both constrained (CD) and non-constrained (NCD) design cases are considered. Considering that ϕ, ψ, Λ vary across the stages, the plotted values in Figures 9 - 12 are the arithmetic averages of the properties across the stages.

To investigate the effect of changing the loading coefficient (ψ) on the performance of the CO_2/C_6F_6 flow path, ψ was varied between 0.8 and 1.5 while fixing the flow coefficient, degree of reaction and pitch to chord ratio to 0.5, 0.5 and 0.85 respectively. For the non-constrained case, denoted by the red line, the loading coefficient was varied between 0.8 and 1.5 for the flow path designed at a loading coefficient of 0.8; where fourteen stages are required to comply with the design criteria. Increasing the ψ results in lower blade velocities hence smaller hub diameter and higher total-to-total efficiency (η_{tt}). The increase in the loading coefficient from 0.8 results in an efficiency increase until a loading coefficient of 1.2 then the efficiency decreases slightly. Further

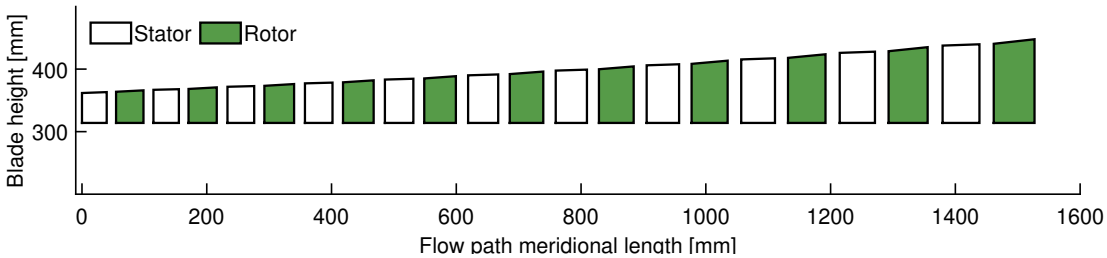

FIGURE 7: TURBINE FLOW PATH MERIDIONAL VIEW FOR THE CO_2/C_6F_6 MIXTURE.

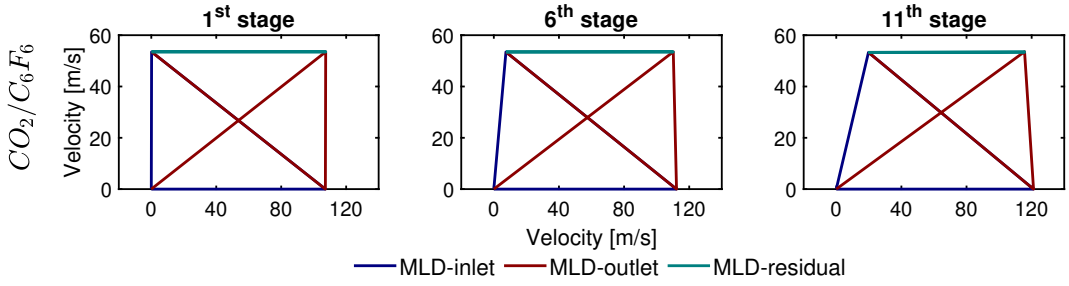

FIGURE 8: VELOCITY TRIANGLES OF THE CO_2/C_6F_6 FLOW PATH.

increase in the loading coefficient results in efficiency reduction as shown in Figure 9.

Increasing the loading coefficient over the range from 0.8 to 1.5 for the constrained turbine design, denoted by the black line, results in higher static bending stresses on the rotor blades and hence, designs accommodate a small number of stages. Reducing the number of stages results in higher peripheral blade speeds, larger hub diameters and hence reduced total-to-total efficiency. From a pure aerodynamic standpoint, increasing the loading coefficient from 0.8 to 1.5 results in an efficiency enhancement of almost 1.1 percentage points. Nonetheless considering the rotor-dynamic and mechanical design constraints, increasing the loading coefficient over the examined range results in efficiency reduction by around 4 percentage points. This significant reduction in the total-to-total turbine (η_{tt}) efficiency is a result of the number of stages reducing from fourteen to five stages to keep the bending stresses within the threshold limit (130 MPa).

To investigate the effect of the flow coefficient (ϕ) on the turbine performance, the analysis has been repeated at a fixed loading coefficient, degree of reaction and pitch-to-chord ratio of 1.0, 0.5 and 0.85 respectively and the flow coefficient was varied between 0.3 and 0.7. For the non-constrained case, denoted by the red line, the flow coefficient was varied between 0.3 and 0.7 for the turbine design produced at a flow coefficient of 0.3; where six stages are required to comply with the design criteria. Increasing ϕ for the same turbine design, for the same number of stages and rotor blades, at the same boundary conditions results in a lower turbine efficiency (Figure 10) owing to the increase in the flow velocities and hence, flow losses.

For the constrained turbine design, donated by the black line, increasing the flow coefficient results in lower bending stresses, and hence allows to accommodate more stages. This results in

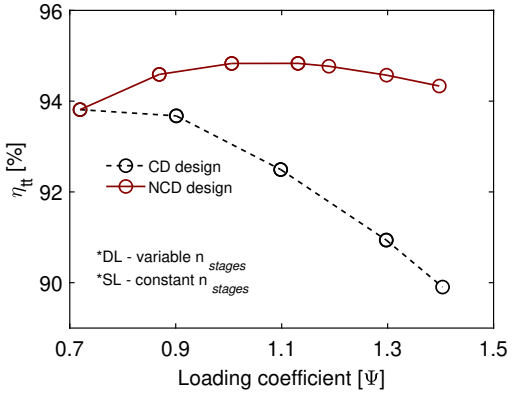

FIGURE 9: THE LOADING COEFFICIENT [ψ] EFFECT ON TOTAL-TO-TOTAL EFFICIENCY [η_{tt}] FOR CONSTRAINED (CD) AND NON-CONSTRAINED DESIGNS (NCD).

smaller hub diameters, and enhanced turbine performance (η_{tt}). This effect is experienced up to an optimum ϕ of 0.5 for a constrained design where afterwards the efficiency deteriorates. Increasing the flow coefficient (ϕ) over the specified range, from 0.3 to 0.7, results in efficiency reduction by up to 2.6%. Nonetheless, taking into account the mechanical and rotor-dyanmic design constraints allows for efficiency enhanced by up to 2.0 percentage points; where the number of stages increases from six to thirteen stages for the C_6F_6 flow path.

As for the effect of the degree of reaction (Figure 11), the non-constrained and constrained designs experience the same effects for increasing the degree of reaction from 0.3 to 0.45; where an efficiency increase is achieved. It is worth noting that the constrained design analysis was carried out for a twelve-

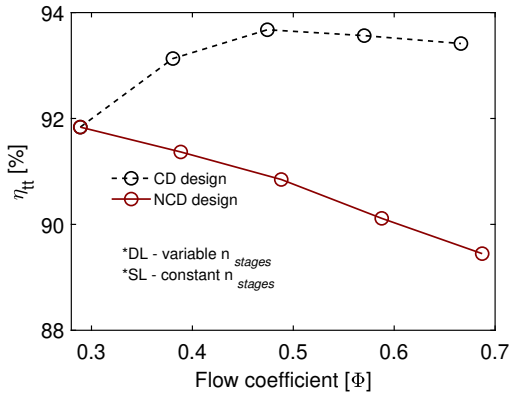

FIGURE 10: THE FLOW COEFFICIENT [ϕ] EFFECT ON TOTAL-TO-TOTAL EFFICIENCY [η_{tt}] FOR CONSTRAINED (CD) AND NON-CONSTRAINED DESIGNS (NCD).

stage design operating at a degree of reaction of 0.3. Increasing the degree of reaction beyond 0.45, for the constrained design, results in higher stresses on the turbine blades due to the higher pressure drop across the rotor blades and hence, less number of design stages and less turbine performance. Increasing the degree of reaction over the specified range results in total-to-total efficiency (η_{tt}) increase by approximately 0.5 percentage points for the constrained turbine design.

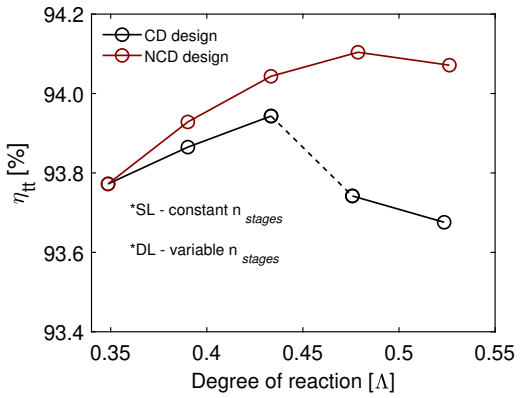

FIGURE 11: THE DEGREE OF REACTION [Λ] EFFECT ON TOTAL-TO-TOTAL EFFICIENCY [η_{tt}] FOR CONSTRAINED (CD) AND NON-CONSTRAINED DESIGNS (NCD).

Furthermore, increasing pitch to chord ratio (s/c) from 0.80 to 0.85 results in better turbine efficiency as indicated in Figure 12 for the non-constrained turbine design due to reducing the blade chord size and hence reducing the tip clearance losses. The effect of changing the pitch-to-chord ratio was investigated for a twelve-stage design produced at a pitch-to-chord ratio of 0.8. The opposite effect is obtained for the constrained turbine design where increasing s/c results in higher bending stress and therefore the design should accommodate less stages. Ultimately, the effect of changing the pitch-to-chord ratio does not have a significant effect on the turbine performance as noticed from the study results due to the narrow range considered for this analysis. Nonetheless, considering a wider range would result in more significant effects.

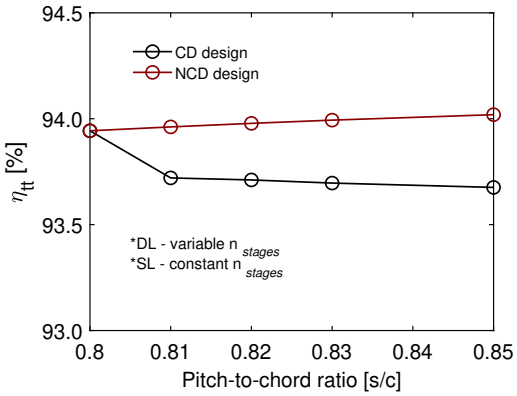

FIGURE 12: THE PITCH-TO-CHORD RATIO [S/C] EFFECT ON TOTAL-TO-TOTAL EFFICIENCY [η_{tt}] FOR CONSTRAINED (CD) AND NON-CONSTRAINED DESIGNS (NCD).

Given that changing both the flow and loading coefficients is found to more significantly affect the performance of the turbine compared to the rest of the design parameters, new flow paths have been designed for the CO_2/C_6F_6 mixture for a range of different loading and flow coefficients (ψ & ϕ). This has been completed at a constant degree of reaction and pitch-to-chord ratio of 0.5 and 0.85 respectively. Figures 13 & 14 reports the resulting stage count and the total-to-total turbine efficiency obtained at different ψ & ϕ values for constrained turbine designs. Increasing the flow coefficient, while keeping the rest of the parameters fixed, means the flow path can accommodate more stages, which increases the efficiency (as indicated in Figure 10). On the contrary, increasing the loading coefficient, while keeping the rest of the parameters fixed, results in fewer turbine stages and less efficiency (as indicated in Figure 9). Combining both effects together, it is observed that by allowing the flow and loading coefficients to vary simultaneously at a fixed degree of reaction and picth-to-chord ratio, it is possible to increase in number of stages in some cases. However, in other cases, the slenderness ratio limits the number of stages as shown in Figures 13 & 14.

By comparing the results obtained at different values of ψ & ϕ to the baseline flow path designed at $\psi = 1.0$ and $\phi = 0.5$, it is observed that a maximum efficiency of 93.8% can be obtained at $\psi = 0.8$ and $\phi = 0.6$. This corresponds to an efficiency enhancement of 0.2%, where the number of stages is increased from fifteen stages compared to eleven stages for the baseline design case. Bearing in mind that increasing the number of stages adds challenges related to the complexity and the cost of the turbine, some consideration of stage number and efficiency enhancement should be should be taken into account. In this capacity, the maps reported in Figures 13 & 14 give an indication of the number of stages needed to achieve high turbine performance. In this regard, to achieve an efficiency greater than 93% (i.e., the yellow area in Figure 14), the turbine should be designed with the number of stages ranging from nine to fifteen; in this range efficiencies of 93.1 & 93.8% are obtained for the designs with nine and fifteen stages designs respectively, with an efficiency difference of 0.69 percentage points.

It is worth mentioning that the same parametric study analysis has been repeated for the CO_2/sCO_2 mixture and the same

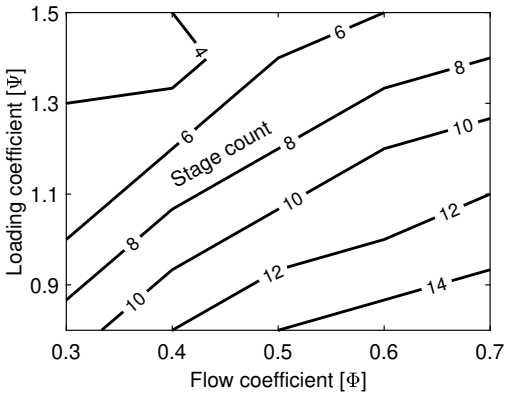

FIGURE 13: STAGE COUNT AT DIFFERENT LOADING [ψ] AND FLOW COEFFICIENTS [ϕ].

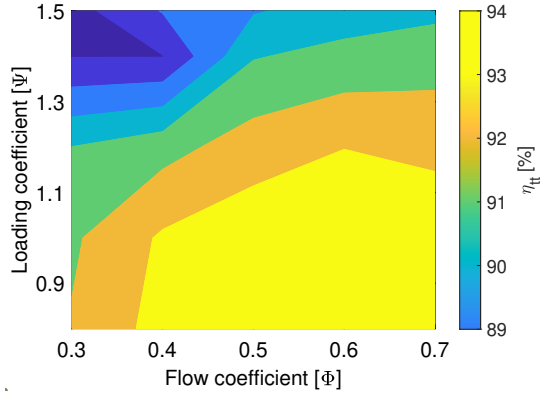

FIGURE 14: TOTAL-TO-TOTAL TURBINE EFFICIENCY [η_{tt}] AT DIFFERENT LOADING [ψ] AND FLOW COEFFICIENTS [ϕ].

conclusions can be drawn. However, some differences are observed in the trends of efficiency with the variation in the flow coefficient. This is due to the CO_2/sCO_2 mixture having a lower sensitivity in the bending stress to the flow coefficient compared to the CO_2/C_6F_6. This is a result of the imposed boundary conditions and differences in the thermo-physical properties of both working fluids.

4. CONCLUSION

Axial turbine flow path designs for a 100 MW_e power plant operating with pure CO_2 and CO_2 mixtures were compared at different operating conditions. This includes designing flow paths for the same cycle configuration and power output, alongside comparing flow paths designed at the same volumetric flow rate and expansion ratio. It was found that turbines operating with both pure CO_2 and CO_2 mixtures result in overall total-to-total efficiencies in excess of 92.5%; where the highest turbine efficiency is achieved for the turbine operating with a pure CO_2. The CO_2/$TiCL_4$ mixture results in the lowest efficiency, with a maximum efficiency that is 1.1 percentage points lower than that of pure CO_2. This is because the CO_2/$TiCL_4$ can only accommodate six stages compared to the thirteen-stages that are possible for pure CO_2. This is due CO_2/$TiCL_4$ design resulting in high rotor bending stresses which is associated with a higher mass flow rate for the same power output. In general, differences in the flow path designs, including the flow path length (number of stages) and turbine geometry, are observed which are due to differences in both the imposed boundary conditions and the properties of the working fluids.

A parametric study was conducted to investigate the effects of changing the aerodynamic design variables, namely the flow coefficient, loading coefficient, degree of reaction and pith-to-chord ratio, on the turbine design and achievable performance, whilst considering the mechanical and rotor-dynamic design aspects. A change in the loading and flow coefficients was found to significantly affect the turbine design when compared to the degree of reaction and pitch-to-chord ratio which showed a lower sensitivity. Increasing the flow coefficient from 0.3 to 0.7, while keeping the loading coefficient, pitch-to-chord ratio and degree of reaction constant at values of 1.0, 0.85 and 0.5 respectively, resulted in an efficiency increase of up to 2.0 percentage points, which is due to being able to increase the number of stages from six to thirteen. Increasing the loading coefficient from 0.8 to 1.5, at a constant flow coefficient, pitch-to-chord ratio and degree of reaction of 0.5, 0.85 and 0.5 respectively, resulted in an efficiency reduction of around four percentage points as a result of having to reduce the number of stages from fourteen to five to comply with the rotordynamic and mechanical design constraints. Changing the flow and loading coefficients simultaneously, whilst maintaining the degree of reaction and pitch-to-chord ratio at values of 0.5 and 0.85 respectively, resulted in an efficiency enhancement of 0.2% with respect to the baseline design produced at loading and flow coefficients of 1.0 and 0.5 respectively. This indicates that modifying key design parameters does not result in significant efficiency enhancements bearing in mind that the 0.2% is within the margin of accuracy of mean-line flow path design.

It is concluded that both CO_2 and CO_2 mixtures result in promising turbine performance with total-to-total efficiencies in excess of 92.5%. Moreover, insignificant differences in aerodynamic performance are observed for turbines operating with CO_2 mixtures compared to those operating with pure CO_2. Ultimately, this indicates that the promising enhancements in the overall plant performance of CO_2 mixtures compared to the pure CO_2 is not hindered by a reduction in the achievable turbine efficiency.

ACKNOWLEDGMENTS

This work was supported by the European Union's Horizon 2020 research and innovation programme under grant agreement Nº814985.

REFERENCES

[1] Crespi, Francesco, de Arriba, Pablo Rodríguez, Sánchez, David and Muñoz, Antonio. "Preliminary investigation on the adoption of CO_2-SO_2 working mixtures in a transcritical Recompression cycle." *Applied Thermal Engineering* Vol. 211 (2022): p. 118384.

[2] "SCARABEUS project Home Page."

[3] Morosini, Ettore, Manzolini, Giampaolo, Di Marcoberardino, Gioele, Invernizzi, Costante and Iora, Paolo. "Investigation of CO_2 mixtures to overcome the limits of sCO_2

cycles." *76th Italian National Congress ATI (ATI 2021)*, Vol. 312: pp. 08010–08019. 2021.

[4] Manzolini, G., Binotti, M., Morosini, E., Sánchez, D., Crespi, F., Di Marcoberardino, G., Iora, P. and Invernizzi, C. "Adoption of CO_2 blended with C_6F_6 as working fluid in CSP plants." *AIP Conference Proceedings*, Vol. 2445. 1: p. 090005. 2022. AIP Publishing LLC. DOI 10.1063/5.0086520.

[5] Rodríguez-deArriba, Pablo, Crespi, Francesco, Sánchez, David, Muñoz, Antonio and Sánchez, Tomás. "The potential of transcritical cycles based on CO_2 mixtures: An exergy-based analysis." *Renewable Energy* Vol. 199 (2022): pp. 1606–1628.

[6] Morosini, Ettore, Ayub, Abubakr, di Marcoberardino, Gioele, Invernizzi, Costante Mario, Iora, Paolo and Manzolini, Giampaolo. "Adoption of the CO_2+ SO_2 mixture as working fluid for transcritical cycles: A thermodynamic assessment with optimized equation of state." *Energy Conversion and Management* Vol. 255 (2022): p. 115263.

[7] Crespi, F, de Arriba, P Rodríguez, Sánchez, D, Ayub, Abubakr, Di Marcoberardino, G, Invernizzi, Costante Mario, Martínez, GS, Iora, Paolo, Di Bona, D, Binotti, Marco et al. "Thermal efficiency gains enabled by using CO_2 mixtures in supercritical power cycles." *Energy* Vol. 238 (2022): p. 121899.

[8] Di Marcoberardino, Gioele, Morosini, Ettore, Di Bona, Daniele, Chiesa, Paolo, Invernizzi, C, Iora, Paolo and Manzolini, Giampaolo. "Experimental characterisation of CO_2+ C_6F_6 mixture: Thermal stability and vapour liquid equilibrium test for its application in transcritical power cycle." *Applied Thermal Engineering* Vol. 212 (2022): p. 118520.

[9] Salah, Salma I., Crespi, Francesco, White, Martin T., noz, Antonio Mu Paggini, Andrea, Ruggiero, Marco, Sánchez, David and Sayma, Abdulnaser I. "Axial turbine flow path design for concentrated solar power plants operating with CO_2 blends." *Submitted:accepted, Applied Thermal Engineering* .

[10] Qi, Jianhui, Reddell, Thomas, Qin, Kan, Hooman, Kamel and Jahn, Ingo H. J. "Supercritical CO_2 Radial Turbine Design Performance as a Function of Turbine Size Parameters." *Journal of Turbomachinery* Vol. 139 No. 8 (2017).

[11] Holaind, Norman, Bianchi, Giuseppe, Miol, Maxence, Sayad Saravi, Samira, Tassou, Savvas, Leroux, Arthur and Jouhara, Hussam. "Design of radial turbomachinery for supercritical CO_2 systems using theoretical and numerical CFD methodologies." Vol. 123: pp. 313–320. 2017. DOI 10.1016/j.egypro.2017.07.256.

[12] Zhou, Aozheng, Song, Jian, Li, Xuesong, Ren, Xiaodong and Gu, Chunwei. "Aerodynamic design and numerical analysis of a radial inflow turbine for the supercritical carbon dioxide Brayton cycle." *Applied Thermal Engineering* Vol. 132 (2018): pp. 245 – 255. DOI https://doi.org/10.1016/j.applthermaleng.2017.12.106.

[13] Lv, Guochuan, Yang, Jinguang, Shao, Wenyang and Wang, Xiaofang. "Aerodynamic design optimization of radial-inflow turbine in supercritical CO_2 cycles using a one-dimensional model." *Energy Conversion and Management* Vol. 165 (2018): pp. 827 – 839. DOI https://doi.org/10.1016/j.enconman.2018.03.005.

[14] Saeed, Muhammad and Kim, Man-Hoe. "Analysis of a recompression supercritical carbon dioxide power cycle with an integrated turbine design/optimization algorithm." *Energy* Vol. 165 (2018): pp. 93 – 111. DOI https://doi.org/10.1016/j.energy.2018.09.058.

[15] Schmitt, J., Willis, Rachel, Amos, D., Kapat, Jayanta and Custer, C. "Study of a Supercritical CO_2 Turbine With TIT of 1350 K for Brayton Cycle With 100 MW Class Output: Aerodynamic Analysis of Stage 1 Vane." *Proceedings of the ASME Turbo Expo* Vol. 3 (2014). DOI 10.1115/GT2014-27214.

[16] Moroz, Leonid, Frolov, Boris, Burlaka, Maksim and Guriev, Oleg. "Turbomachinery Flowpath Design and Performance Analysis for Supercritical CO_2." *Proceedings of the ASME Turbo Expo: Turbine Technical Conference and Exposition*. June 16–20, 2014, Düsseldorf, German.

[17] Zhang, Hanzhen, Zhao, Hang, Deng, Qinghua and Feng, Zhenping. "Aerothermodynamic Design and Numerical Investigation of Supercritical Carbon Dioxide Turbine." *Proceedings of the ASME Turbo Expo: Turbine Technical Conference and Exposition*. June 15–19, 2015, Montreal, Quebec, Canada.

[18] Shi, Dongbo, Zhang, Lei, Xie, Yong and Zhang, Di. "Aerodynamic Design and Off-design Performance Analysis of a Multi-Stage S-CO_2 Axial Turbine Based on Solar Power Generation System." *Applied Sciences* Vol. 9 (2019): p. 714. DOI 10.3390/app9040714.

[19] Clementoni, Eric M., Cox, Timothy L. and King, Martha A. "Off-Nominal Component Performance in a Supercritical Carbon Dioxide Brayton Cycle." *Journal of Engineering for Gas Turbines and Power* Vol. 138 No. 1 (2015). DOI 10.1115/1.4031182.

[20] Utamura, Motoaki, Hasuike, Hiroshi, Ogawa, Kiichiro, Yamamoto, Takashi, Fukushima, Toshihiko, Watanabe, Toshinori and Himeno, Takehiro. "Demonstration of Supercritical CO_2 Closed Regenerative Brayton Cycle in a Bench Scale Experiment." *Proceedings of the ASME Turbo Expo: Turbine Technical Conference and Exposition*. June 11–15, 2012, Copenhagen, Denmark.

[21] Wright, Steven Alan, Radel, Ross F, Vernon, Milton E, Pickard, Paul S and Rochau, Gary Eugene. "Operation and analysis of a supercritical CO_2 Brayton cycle." Technical report no. Sandia National Laboratories (SNL), Albuquerque, NM, and Livermore, CA. 2010.

[22] Kimball, Kenneth J. and Clementoni, Eric M. "Supercritical Carbon Dioxide Brayton Power Cycle Development Overview." *Proceedings of the ASME Turbo Expo: Turbine Technical Conference and Exposition*. June 11–15, 2012, Copenhagen, Denmark.

[23] Cho, Junhyun, Shin, Hyungki, Ra, Ho-Sang, Lee, Gilbong, Roh, Chulwoo, Lee, Beomjoon and Baik, Young-Jin. "Development of the Supercritical Carbon Dioxide Power Cycle Experimental Loop in KIER.": p. V009T36A013. 2016. DOI 10.1115/GT2016-57460.

[24] Moore, Jeff, Brun, Klaus, Evans, Neal and Kalra, Chiranjeev. "Development of 1 MWe Supercritical CO_2 Test Loop." *Proceedings of ASME Turbomachinery Technical Conference and Exposition*. June 15–19, 2015, Montreal, Quebec, Canada.

[25] Dostal, V., Driscoll, M.J. and Hejzlar, P. *A supercritical carbon dioxide cycle for next generation nuclear reactors*. Massachusetts Institute of Technology, Boston, MA. (2004).

[26] R.Bidkar, G.Musgrove,M. Day,C.Kulhanek, T.Allison. "Conceptual Designs of 50 MWe and 450 MWe Supercritical CO_2 Turbomachinery Trains for Power Generation from Coal. Part 2: Compressors." 5th *Int. Symp. - Supercrit. CO_2 Power Cycles*: pp. 1–18. March 28-31, 2016, San Antonio, Texas.

[27] Allison, T.C., Moore, J., Pelton, R., Wilkes, J. and Ertas, B. "7 - Turbomachinery." Brun, Klaus, Friedman, Peter and Dennis, Richard (eds.). *Fundamentals and Applications of Supercritical Carbon Dioxide (sCO_2) Based Power Cycles*. Woodhead Publishing (2017): pp. 147 – 215. DOI https://doi.org/10.1016/B978-0-08-100804-1.00007-4.

[28] Salah, Salma I, Khader, Mahmoud A, White, Martin T and Sayma, Abdulnaser I. "Mean-line design of a supercritical CO_2 micro axial turbine." *Applied Sciences* Vol. 10 No. 15 (2020): p. 5069.

[29] Salah, Salma I., White, Martin T. and Sayma, Abdulnaser I. "A comparison of axial turbine loss models for air, sCO_2 and ORC turbines across a range of scales." *International Journal of Thermofluids* (2022): p. 100156DOI https://doi.org/10.1016/j.ijft.2022.100156.

[30] Aungier, Ronald H. *Turbine Aerodynamics: Axial-Flow and Radial-Flow Turbine Design and Analysis*. ASME Press (2006). DOI 10.1115/1.802418.

[31] Dixon, S.L. and Hall, C.A. "Chapter 4 - Axial-Flow Turbines: Mean-Line Analysis and Design." Dixon, S.L. and Hall, C.A. (eds.). *Fluid Mechanics and Thermodynamics of Turbomachinery*, sixth edition ed. Butterworth-Heinemann, Boston (2010): pp. 97 – 141. DOI https://doi.org/10.1016/B978-1-85617-793-1.00004-3.

[32] Abdeldayem, Abdelrahman S., Salah, Salma I., Aqel, Omar, White, Martin T. and Sayma, Abdulnaser I. "Design of a 130 MW axial turbine operating with a supercritical carbon dioxide mixture for the SCARABEUS project." 15th *European Turbo-machinery conference*. 24-28th April 2023, Budapest, Hungry.

[33] Dias, Ana MA, Carrier, Herve, Daridon, Jean L, Pamies, Josep C, Vega, Lourdes F, Coutinho, Joao AP and Marrucho, Isabel M. "Vapor- liquid equilibrium of carbon dioxide- perfluoroalkane mixtures: experimental data and SAFT modeling." *Industrial & engineering chemistry research* Vol. 45 No. 7 (2006): pp. 2341–2350.

[34] Tolley, WK, Izatt, RM and Oscarson, JL. "Titanium tetrachloride-supercritical carbon dioxide interaction: A solvent extraction and thermodynamic study." *Metallurgical Transactions B* Vol. 23 No. 1 (1992): pp. 65–72.

[35] Coquelet, C., Valtz, A. and Arpentinier, P. "Thermodynamic study of binary and ternary systems containing CO_2+ impurities in the context of CO_2 transportation." *Fluid Phase Equilibria* Vol. 382 (2014): pp. 205–211. DOI https://doi.org/10.1016/j.fluid.2014.08.031.

[36] Aqel, Omar A, White, Martin T, Khader, MA and Sayma, AI. "Sensitivity of transcritical cycle and turbine design to dopant fraction in CO_2-based working fluids." *Applied Thermal Engineering* Vol. 190 (2021): p. 116796.

[37] Manzolini, Giampaolo, Binotti, Marco, Bonalumi, Davide, Invernizzi, Costante and Iora, Paolo. "CO_2 mixtures as innovative working fluid in power cycles applied to solar plants. Techno-economic assessment." *Solar Energy* Vol. 181 (2019): pp. 530 – 544. DOI https://doi.org/10.1016/j.solener.2019.01.015.

[38] Marcoberardino, G. Di, Morosini, E., Bonac, D. Di, Chiesabc, P., Invernizzia, C., Ioraa, P. and Manzolin, G. "Experimental characterisation of CO_2 + C_6F_6 mixture: thermal stability and vapour liquid equilibrium test for its application in transcritical power cycle." *Applied Thermal Engineering* Vol. 212 (2022): p. 118520.

[39] Smith, S. F. "A Simple Correlation of Turbine Efficiency." *The Journal of the Royal Aeronautical Society* Vol. 69 No. 655 (1965): p. 467–470. DOI 10.1017/S0001924000059108.

[40] Kacker, S. C. and Okapuu, U. "A Mean Line Prediction Method for Axial Flow Turbine Efficiency." *Journal of Engineering for Power* Vol. 104 No. 1 (1982): pp. 111–119. DOI 10.1115/1.3227240.

[41] Moustapha, H., Zelesky, M.F., Balnes, N.C. and Japikse, D. "Chapter 3 - Preliminary and through flow design." *Axial and Radial Turbines*. Concepts NREC (2003): pp. 65–95.

[42] Lee, Jekyoung, Lee, Jeong Ik, Ahn, Yoonhan and Yoon, Hojoon. "Design Methodology of Supercritical CO_2 Brayton Cycle Turbomachineries." *Proceedings of the ASME Turbo Expo: Turbine Technical Conference and Exposition*. June 11–15, 2012, Copenhagen, Denmark.

[43] Balje, O. E. and Binsley, R. L. "Axial Turbine Performance Evaluation. Part A—Loss-Geometry Relationships." *Journal of Engineering for Power* Vol. 90 No. 4 (1968): pp. 341–348. DOI 10.1115/1.3609211. URL https://asmedigitalcollection.asme.org/gasturbinespower/article-pdf/90/4/341/5720173/341_1.pdf.

[44] Soderberg, C. R. *Gas Turbine Laboratory, Massachusetts Institute of Technology* (1949)DOI 10.1115/90-GT-150.